ARKIV FÖR FYSIK Band 12 nr 23

Communicated 11 September 1957 by MANNE SIEGBAHN and ERIK HULTHÉN

Applications of a multi-channel goniometer

By TORSTEN LINDQVIST and ERIK KARLSSON

With 11 figures in the text

SUMMARY

A multi-channel goniometer (MCG) for gamma-gamma angular correlation measurements is described. The apparatus has four channels. Various methods of measurement and a complete treatment of data are given. The MCG has been carefully tested with well known correlations (Bi^{207}, Hf^{181} and Co^{60}). As applications the angular correlations of gamma cascades from Ba^{131} and Nd^{147} have been investigated. Both cases involve l-forbidden magnetic dipole transitions. From the mixing ratios determined in the correlation experiments it is possible to estimate the strength of forbiddenness. An upper limit of the g-factor of the 92 keV level in Pm^{147} is determined by studying the influence of a magnetic field on the angular correlation.

1. Introduction

Recently an apparatus for angular correlation measurements was described [1] in which four detectors were used instead of two detectors. The basic idea was to record the coincidences between any two of these four detectors simultaneously. The main advantage of such an arrangement is the increased coincidence efficiency. In this paper will be given some details of the construction, various methods of measurement, complete treatment of data, and applications.

In ref. [1] the apparatus was named the "Multi-Coincidence Goniometer". The expression "multi-coincidence" is not suitable because it may refer to triple and quadruple coincidences, which are not wanted in this apparatus. A more adequate name is "Multi-Channel Goniometer" (MCG).

2. The Block Diagram

How the MCG works has been described in detail elsewhere [1]. A short description will be given here.

The four detectors each consisting of a NaI(Tl) crystal, a photomultiplier and a cathode follower, view the same source (Fig. 1). From the linear amplifier in each channel (cf. block diagram, Fig. 2) the pulse spectrum is fed into a limiting amplifier and then into a fast coincidence unit.

When pulses from any two counters are in coincidence the fast coincidence unit delivers an output pulse to a "conditioned gate" in each channel.

From the gates the pulses go to a "coincidence matrix", which determines between which two counters the coincidence has occurred. The unit delivers output pulses to two rows each of six terminals.

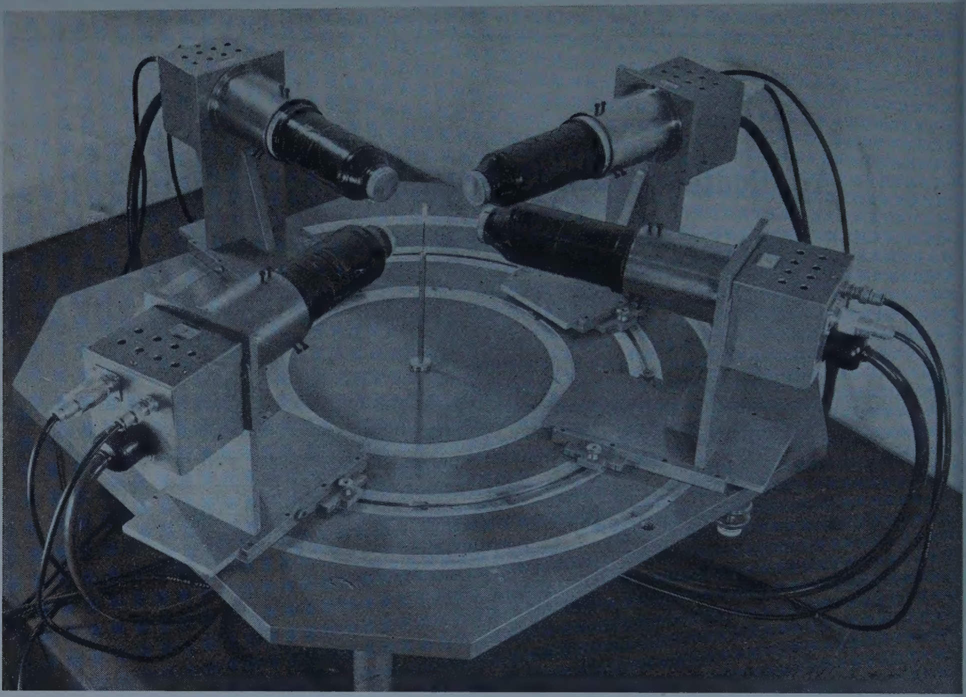

Fig. 1. The four scintillation detectors of the MCG.

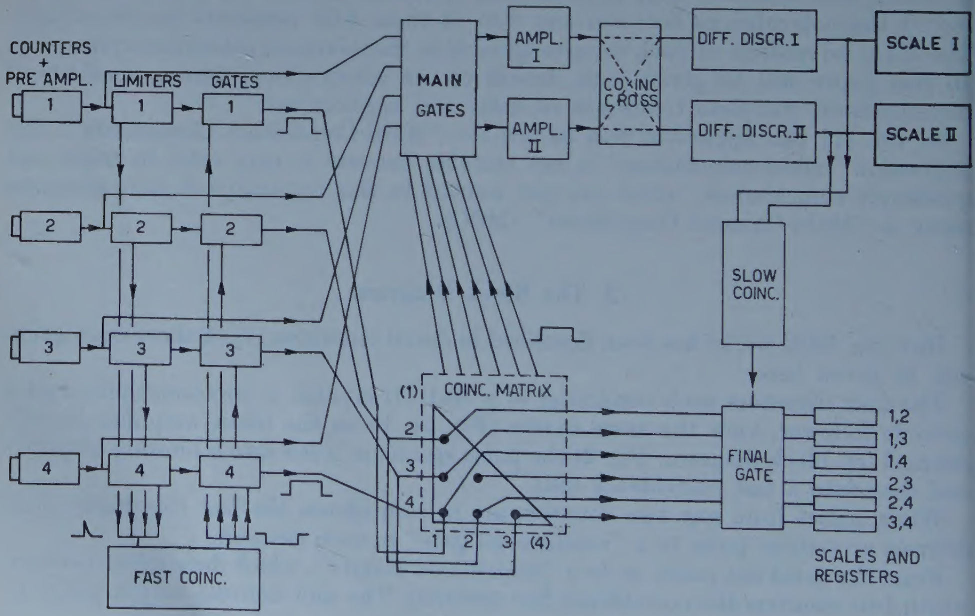

Fig. 2. Block diagram of the MCG.

The first row is connected to the final gate. Each pair combination of the detectors corresponds to a terminal of this row.

The second row is connected to the main gate, where it gates the two coincident pulses into two channels for energy selection.

This energy selection takes place in an ordinary two-channel coincidence spectrometer with differential discriminators. However, as shown in the block diagram (Fig. 2) a "coincidence cross delay" is introduced. This arrangement improves the coincidence counting efficiency by a factor of two. From the output of the slow coincidence unit, signals are fed to the final gate.

The final gate transmits the pulses from the coincidence matrix to the register units provided there comes a pulse from the slow coincidence unit. Thus, for each detector pair combination, there is obtained the number of coincidences that have fulfilled the energy condition set by the differential discriminators. These coincidences are recorded on six register units representing the combinations 12, 13, 14, 23, 24 and 34.

3. Some details of the construction

(*a*) *Limiter potentiometers.*—The problem of triple coincidences is of importance in the MCG. In many decay schemes there is an X-ray (or another gamma ray) in coincidence with the double gamma cascade of interest, and this fact can lead to triple coincidences. For instance the fast coincidence unit can be triggered by a gamma combination of which one gamma ray does not fulfill the energy conditions. Then, within the resolving time of the slow coincidence unit, a third gamma ray with the proper energy can appear and this gives rise to false coincidences in three combinations. This effect can be considerably decreased by the limiters. By attenuating potentiometers in the limiters the minimum pulse height for giving an output pulse can be adjusted. Thus it is possible to cut off completely the low energy part of the spectrum and the triple coincidence effect becomes negligible.

(*b*) *Cross delay.*—The cross delay is of LC-type. The delay time was originally 3 μs in each channel. However, in the presence of a very large pulse the differential discriminators could be blocked for the small pulse that followed after 3 μs. Therefore the delay time was increased to 6 μs. The small spectrum distortion that is introduced by the MCG and the cross delay is demonstrated in Fig. 3. The curve *a* shows the single gamma ray spectrum of Bi^{207}, taken with one detector followed by a linear amplifier and a differential discriminator. The curve *b* shows the same spectrum, now passed through the MCG and the cross delay. The curve *b* is a combination of six coincidence spectra of which three have passed directly from AMPL I to DIFF. DISCR. I (Fig. 2) and three have been "crossed" from AMPL. II to DIFF. DISCR. I. The curve *b* is taken at the output of the discriminator I (Fig. 2).

(*c*) *Single spectra through the MCG.*—In order to adjust the over-all amplification of each channel so that the four gamma ray spectra overlap, it is necessary to be able to measure the single spectrum from each detector through the MCG. Also for evaluating the number of accidental coincidences in each combination it is necessary to know the single counting rates. The single spectra from one detector through the MCG is obtained if the same detector is connected in parallel also to another limiter. One then gets artificial coincidences of the same number as the single counts. In practice a special switch is introduced (not shown in Fig. 2), where it is possible to make the necessary connections only by turning the switch.

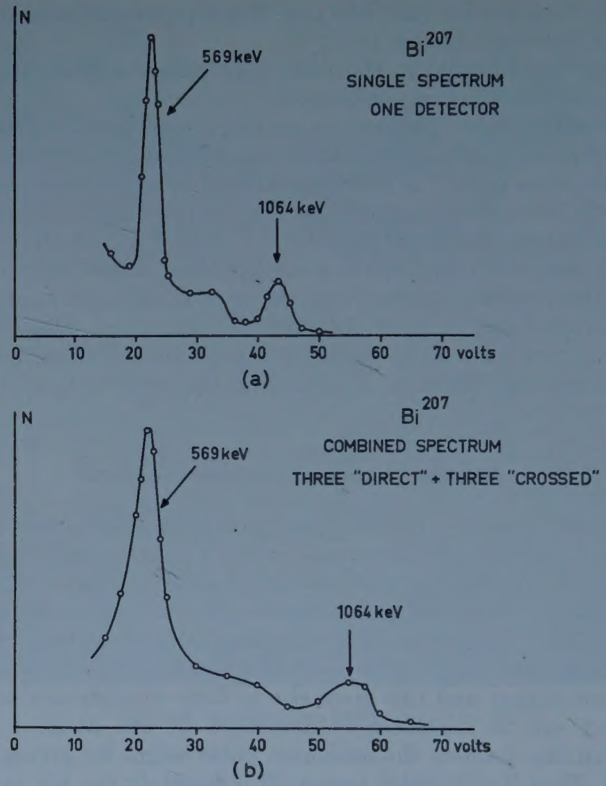

Fig. 3. Gamma ray spectrum of Bi^{207}, (*a*) single spectrum from one detector, (*b*) coincidence spectrum through the MCG and the cross delay.

4. Methods of measurement

In angular correlation experiments one determines the coefficients A_ν in the correlation function

$$W(\theta) = \sum A_\nu P_\nu \; (\cos \theta) \qquad \nu = 0, 2, 4. \tag{1}$$

The coefficients A_ν depend on the spins and the multipolarities of the gamma cascade. The number of terms in $W(\theta)$ is determined by

$$\nu_{\max} \leq \min(2I_b, 2L_1, 2L_2), \tag{2}$$

where I_b is the spin of the intermediate level and L_1 and L_2 are the multipolarities of the gamma cascade.

The minimum number of angles θ to be measured if a complete knowledge of the correlation function $W(\theta)$ is wanted, is determined by eq. (2).

For the MCG measurements there are various angular arrangements of the detectors available. Depending on eq. (2) for the actual case one or two of these arrangements are used.

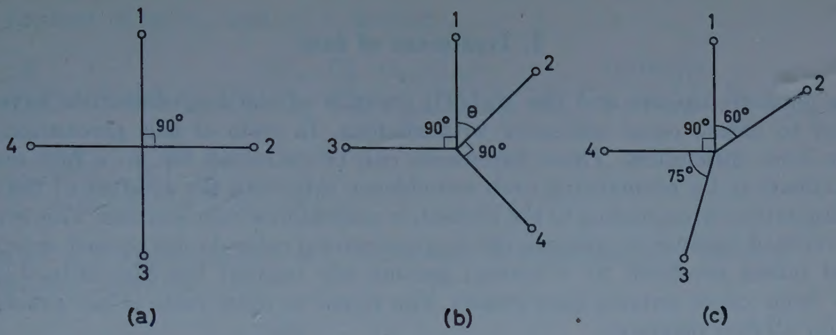

Fig. 4. Geometrical arrangements of the four detectors, (*a*) symmetric, (*b*) semi-symmetric and (*c*) asymmetric.

(*a*) The symmetric arrangement (Fig. 4*a*) is the simplest and most often used. Only the angles 180° and 90° are measured. The angle 180° appears twofold and 90° fourfold. From these two angles the anisotropy A is obtained:

$$A = \frac{W(180) - W(90)}{W(90)} \tag{3}$$

The anisotropy A gives all information necessary if $\nu_{\max} = 2$, i.e. when $I_b \leq \frac{3}{2}$ and/or one of the gamma radiations is pure dipole according to eq. (2).

In many cases it is of interest to study how the angular correlation depends on the chemical or physical form of the source or on an external magnetic field. Then the anisotropy A gives the answer even when $\nu_{\max} > 2$.

When the source is a positron emitter, A does not give a good answer since the coincidence rate at 180° is enhanced through the annihilation radiation.

(*b*) The semi-symmetric arrangement (Fig. 4*b*) is in many cases complementary to the arrangement *a*. The angle θ is mostly 45° and the angles measured are 45°, 90° and 135°. In this arrangement 45° (135°) appears fourfold and 90° twofold. From these angles one obtains the anisotropy U defined as

$$U = \frac{W(135) - W(90)}{W(90)} \tag{4}$$

When A and U are known one can calculate the coefficients A_2 and A_4 in $W(\theta)$.

The angle $\theta = 60°$ can also be used. One obtains then the anisotropy V defined as

$$V = \frac{W(120) - W(90)}{W(90)} \tag{5}$$

In the case of a positron emitter and when $\nu_{\max} = 4$, U and V are the quantities necessary for calculating A_2 and A_4 in the correlation function $W(\theta)$.

(*c*) The asymmetric arrangement (Fig. 4*c*) uses six different angles, namely 60°, 75°, 90°, 135°, 150° and 165°, each angle onefold. Since the number of angles θ now is larger than the number of terms in the correlation function one uses a least square fit for calculating the coefficients A_2 and A_4. It will be shown below that this method is not as accurate as arrangements *a* and *b*.

5. Treatment of data

The photomultipliers and the NaI(Tl) crystals of the four detectors have been selected to obtain equal efficiency with all four. In spite of this precaution there remain some differences. These differences can be corrected for, to a first order of approximation, by normalizing each coincidence rate with the product of the single counting rates corresponding to the respective coincidence combination. This is not an exact method because, in general, the single counting rates do not consist only of the desired pulses produced by a certain gamma ray (signal) but also of background pulses from other gamma rays (noise). The signal to noise ratio is not exactly the same for all four detectors.

(*a*) There is, however, a more accurate method. Let C_{ij} be the number of coincidences between gamma ray A in detector i and gamma ray B in detector j ($j > i$; $i,j = 1,2,3,4$). Due to the action of the "cross delay", coincidences between gamma ray A in detector j and gamma ray B in detector i will also be recorded and are marked C^*_{ji}. The coincidence rates then become

$$C_{ij} = \frac{N'_{iA} \cdot N'_{jB}}{N_0} \; f(\theta), \tag{6}$$

$$C^*_{ji} = \frac{N'_{jA} \cdot N'_{iB}}{N_0} \; f(\theta), \tag{7}$$

where N'_{iA} etc. is the number of pulses from gamma ray A in detector i, etc. N_0 is the total source strength and $f(\theta)$ is the angular correlation function. Because of the construction of the main gate, the pulses from detectors 2 and 3 can each go different ways according to the combination in which they appear. Thus one has $N'_{2'A}$ and $N'_{2''A}$, $N'_{3'A}$ and $N'_{3''A}$, and the corresponding numbers for the gamma ray B. With the symmetric arrangement (Fig. 4*a*) one has the following coincidence rates:

$$\left.\begin{array}{ll} C_{12} = \dfrac{N'_{1A} \cdot N'_{2''B}}{N_0} \; f(90); & C_{23} = \dfrac{N'_{2'A} \cdot N'_{3''B}}{N_0} \; f(90) \\[2ex] C_{13} = \dfrac{N'_{1A} \cdot N'_{3''B}}{N_0} \; f(180); & C_{24} = \dfrac{N'_{2'A} \cdot N'_{4B}}{N_0} \; f(180) \\[2ex] C_{14} = \dfrac{N'_{1A} \cdot N'_{4B}}{N_0} \; f(90); & C_{34} = \dfrac{N'_{3'A} \cdot N'_{4B}}{N_0} \; f(90) \end{array}\right\} \tag{8}$$

and the corresponding expressions for the "crossed" coincidence rates C^*_{ji}, where A and B interchange.

The following ratios are formed:

$$a_{iA} = \frac{C_{ik}}{C_{ij}} \quad \text{and} \quad a_{iB} = \frac{C_{ki}}{C_{ji}} \tag{9}$$

where $ijk = 123,\ 234,\ 341,\ 412.$

The product of all a_{iA} and a_{iB} is formed

$$\prod_{i=1}^{4}(a_{iA}\cdot a_{iB})=\frac{(C_{13}\cdot C_{31}^{*}\cdot C_{24}\cdot C_{42}^{*})^{2}}{C_{12}\cdot C_{21}^{*}\cdot C_{23}\cdot C_{32}^{*}\cdot C_{34}\cdot C_{43}^{*}\cdot C_{14}\cdot C_{41}^{*}}=\left[\frac{f(180)}{f(90)}\right]^{8}\cdot n, \tag{10}$$

where $n=\left[\frac{N'_{3''}\cdot N'_{2'}}{N'_{3'}\cdot N'_{2''}}\right]_{A}\cdot\left[\frac{N'_{3''}\cdot N'_{2'}}{N'_{3'}\cdot N'_{2''}}\right]_{B}$.

The factor n is approximately $=1$, which can be experimentally verified.

As defined above [eq. (3)]

$$\frac{f(180)}{f(90)}-1=\text{the anisotropy } A. \tag{11}$$

Accordingly, from eq. (10), when $\sqrt[8]{n}=1$,

$$A=\sqrt[8]{\frac{(C_{13}\cdot C_{31}^{*}\cdot C_{24}\cdot C_{42}^{*})^{2}}{C_{12}\cdot C_{21}^{*}\cdot C_{23}\cdot C_{32}^{*}\cdot C_{34}\cdot C_{43}^{*}\cdot C_{14}\cdot C_{41}^{*}}}-1. \tag{12}$$

In the MCG one does not register the "direct" (C_{ij}) and the "crossed" (C_{ji}^{*}) coincidences separately, but the sum of them ($C_{ij}+C_{ji}^{*}$). However, eq. (12) can to a very good approximation be written as

$$A=\sqrt[4]{\frac{C_{13}^{2}\cdot C_{24}^{2}}{C_{12}\cdot C_{23}\cdot C_{34}\cdot C_{14}}}-1, \tag{13}$$

where now C_{ij} stand for the sum ($C_{ij}+C_{ji}^{*}$) and are the six coincidence combinations recorded on the registers.

With the semi-symmetric arrangement (Fig. 4*b*, note the order of detectors: 1,2, 4,3) exactly the same analysis can be carried out as for the symmetric arrangement. When $\theta=45°$ one obtains the anisotropy U as

$$U=\sqrt[4]{\frac{C_{12}\cdot C_{23}\cdot C_{34}\cdot C_{14}}{C_{13}^{2}\cdot C_{24}^{2}}}-1 \tag{14}$$

and a similar expression for the anisotropy V when $\theta=60°$.

(*b*) An exact method can be applied if C_{12} and C_{34} are excluded from the treatment. For the "direct" coincidences one then obtains according to eqs. (8)

$$\frac{C_{13}\cdot C_{24}}{C_{14}\cdot C_{23}}=\left[\frac{f(180)}{f(90)}\right]^{2}. \tag{15}$$

Eqs. (11) and (15) then give

$$A=\sqrt{\frac{C_{13}\cdot C_{24}}{C_{14}\cdot C_{23}}}-1. \tag{16}$$

The corresponding treatment for the anisotropy U (Fig. 4*b*) gives

$$U=\sqrt{\frac{C_{14}\cdot C_{23}}{C_{13}\cdot C_{24}}}-1. \tag{17}$$

(*c*) The asymmetric arrangement (Fig. 4*c*) cannot be treated with the above-mentioned methods. It is here necessary to normalize the coincidence rates with the single counting rates.

$$C_{ij,\,\mathrm{norm}}=\frac{C_{ij}}{N_{iA}\cdot N_{jB}+N_{jA}\cdot N_{iB}}. \tag{18}$$

The single counting rates N_{2A} etc. can easily be measured according to Chap. 3*c*. $C_{ij,\,\mathrm{norm}}$ are then fitted to the correlation function $W(\theta)$ with a least square method.

6. Corrections

The corrections, which have to be applied in an MCG-measurement, are the same as in an ordinary angular correlation measurement.

(*a*) The numbers of accidental coincidences in each combination are determined according to the relation

$$C_{ij,\,\mathrm{acc}}=2\,\tau_{ij}\,(N_{iA}\cdot N_{jB}+N_{jA}\cdot N_{iB}). \tag{19}$$

τ_{ij} are the resolving times of the respective combinations. The resolving times were measured with oscilloscope and with the technique of two independent radioactive sources and were found to vary from 0.49 μs to 0.67 μs. It is somewhat surprising that τ_{ij} is not a constant for all combinations. The reason might be the different counters and linear amplifiers in the combinations.

(*b*) The correction for the counter solid angle has been determined according to a method proposed by Lawson and Frauenfelder [2]. The energies investigated were 0.661 MeV (Cs^{137}) and 1.33 MeV (Co^{60}) and the correction was determined for two distances between source and detector, 5 cm and 10 cm. For distances between 5 and 10 cm one can interpolate.

(*c*) The problem of scattering from one detector to another is usually not serious, since only the photopeaks of each gamma ray are recorded. Lead blocks, one in. thick, have been used between the detectors, but they did not have any influence on the measurements.

7. Applications

(*a*) *Bi^{207}, Hf^{181} and Co^{60}.*—The decay schemes are well established (Fig. 5) and the angular correlation functions are determined to a high degree of accuracy. Therefore these cases are well suited as tests of the MCG. The angular correlation of the 1.064–0.569 MeV cascade from Bi^{207} was determined by McGowan and Campbell [3], the 0.133–0.482 MeV cascade from Hf^{181} by McGowan [4] and also by Heer *et al.* [5]. Finally, the angular correlation of the 1.17–1.33 MeV cascade from Co^{60} was determined by Klema and McGowan [6] and also by Lawson and Frauenfelder [2].

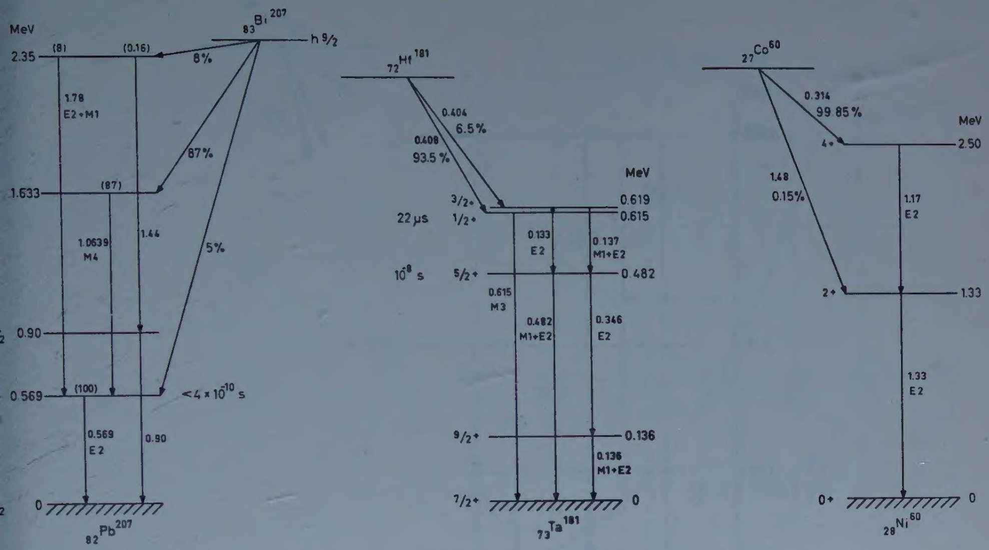

Fig. 5. Decay schemes of Bi^{207} (ref. [23]), Hf^{181} (ref. [24]) and Co^{60} (ref. [25]).

The results of the runs with Bi^{207}, Hf^{181} and Co^{60} are shown in Table 1. The previous measurements are also given for comparison. Thus it is shown that the MCG works properly.

(*b*) *Ba*^{131}.—The decay scheme of Ba^{131} (Fig. 6) was determined by H. Vartapetain [7]. Ba^{131} ($T_{1/2} = 11.5\ d$) decays by electron capture to excited states in Cs^{131}. The capture transition to the ground state of Cs^{131} has not been found. The 122 keV transition occurs between $g_{7/2}$ and $d_{5/2}$ levels and is an l-forbidden $M1$ transition ($\Delta l = 2$, $\Delta j = 1$). The conversion coefficient of the 122 keV transition indicates that it is pure $M1$ [7]. An angular correlation measurement with the 122 keV gamma ray should reveal any presence of $E2$.

The halflife of the 122 keV level has been measured by H. Vartapetain *et al.* [8] to be $(4.0 \pm 0.3) \cdot 10^{-9}$ s.

Table 1. Results of the correlation experiments on Bi^{207}, Hf^{181} and Co^{60}.

Isotope source	Detector arrangement	Treatment of data	Result A and U	Result A_2 and A_4	Previous measurement	Ref.
Bi^{207} solid	Fig. 4 *a* Fig. 4 *b*	Eq. (13) Eq. (17)	$A = +0.342 \pm 0.030$ $U = +0.188 \pm 0.028$	$A_2 = +0.022 \pm 0.016$ $A_4 = -0.016 \pm 0.024$	$A_2 = +0.2208$ $A_4 = -0.0180$	[3]
Hf^{181} HfF_4 solution	Fig. 4 *a* Fig. 4 *b*	Eq. (16) Eq. (17)	$A = -0.332 \pm 0.017$ $U = -0.102 \pm 0.020$	$A_2 = -0.230 \pm 0.012$ $A_4 = -0.080 \pm 0.020$	$A_2 = -0.280$ $A_4 = -0.057$	[4]
Co^{60} CoCl solid	Fig. 4 *a* Fig. 4 *b*	Eq. (13) Eq. (14)	$A = +0.148 \pm 0.015$ $U = +0.061 \pm 0.015$	$A_2 = +0.096 \pm 0.009$ $A_4 = +0.012 \pm 0.015$	$A_2 = +0.1020$ $A_4 = +0.0096$	[6]

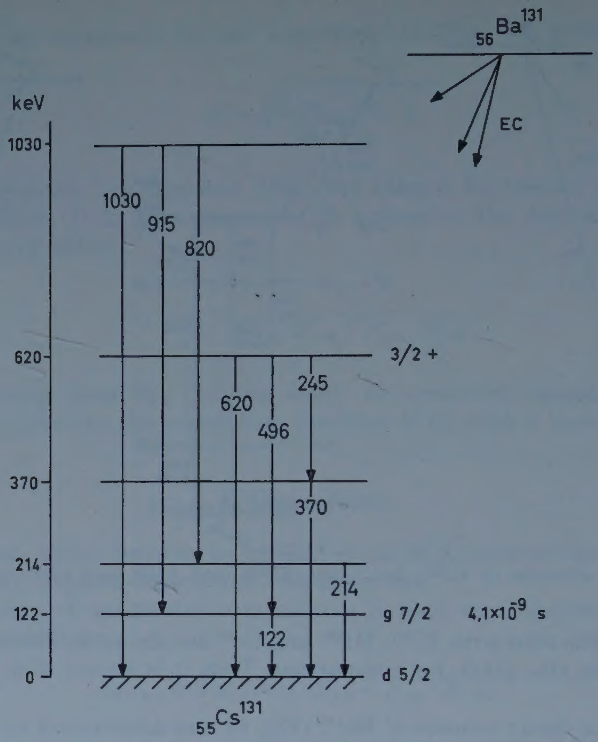

Fig. 6. Decay scheme of Ba^{131}.

The barium activity was produced by bombarding caesium chloride with 42 MeV protons in the synchrocyclotron of the Werner Institute, Uppsala. The reaction was $Cs^{133}(p,3n)Ba^{131}$. The isomeric Ba^{133m} ($T_{1/2} = 35$ h) was also produced but after a few days it did not disturb the measurements. The caesium chloride was dissolved in acetic acid and the barium was precipitated as barium chromate. The barium activity was then precipitated as barium chloride dissolved in hydrochloric acid. In this form it was used for the angular correlation measurements.

It is of importance to have the source in solution because of the lifetime of the intermediate level. In a solid source one can expect extranuclear effects, which can attenuate the correlation.

The angular correlation of the 496–122 keV cascade was investigated. The 496 keV transition is a quadrupole transition between $3/2+$ and $7/2+$ states. Thus no dipole admixture is possible and no octopole admixture is expected. The high energy transition in coincidence with the 122 keV line is of very low intensity and the coincidences can be neglected.

The anisotropies A and U were determined and the data were treated according to eqs. (16) and (17). The results were

$$A = +0.0100 \pm 0.0038, \qquad U = +0.0067 \pm 0.0038.$$

After correction for counter solid angle the following correlation function was obtained

$$W(\theta) = 1 + (0.007 \pm 0.002) P_2(\cos\theta) - (0.002 \pm 0.004) P_4(\cos\theta).$$

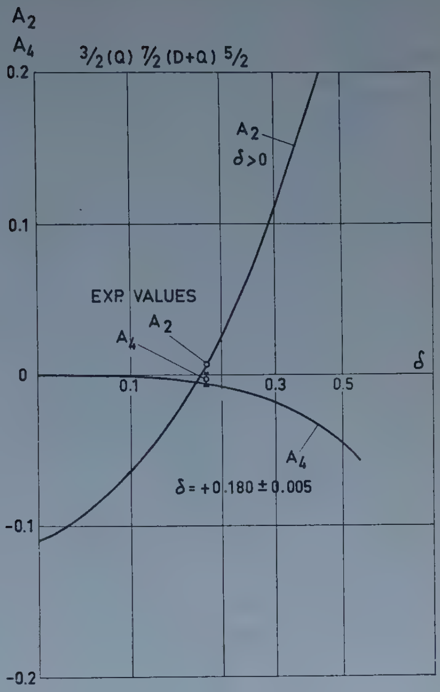

Fig. 7. A_2 and A_4 as functions of the mixing parameter δ in the spin sequence $3/2\,(Q)\,7/2\,(D+Q)\,5/2$.

The 496–122 keV cascade represents the spin sequence $3/2(Q)7/2(D+Q)5/2$. The coefficients A_2 and A_4 as functions of δ, the mixing parameter of the 122 keV transition, are given in Fig. 7. The experimental values of A_2 and A_4 define

$$\delta_{122} = +0.180 \pm 0.005.$$

It is therefore concluded that the 122 keV transition in Cs^{131} is

$$(97 \pm 1)\,\%\,M1 + (3 \pm 1)\,\%\,E2.$$

(c) *Nd*^{147}.—The decay scheme of Nd^{147} (Fig. 8) was determined by Hans *et al.* [9]. Nd^{147} ($T_{1/2} = 11\ d$) decays by beta emission to excited states in Pm^{147}. The ground state of Pm^{147}, which decays to Sm^{147}, was given the spin $d_{5/2}$ from the first forbidden character of the beta-transition. The absence of a beta-transition to the ground state of Pm^{147} suggests that the ground state of Nd^{147} is $h_{9/2}$. Conversion data identify the 92 keV transition as $M1$ and the spin of the 92 keV-level was taken as $g_{7/2}$. Accordingly the 92 keV transition occurs between $g_{7/2}$ and $d_{5/2}$ levels and is an l-forbidden $M1$ transition.

The halflife of the 92 keV level was measured by Graham and Bell [10] to be 2.44×10^{-9} s.

Ambler *et al.* [11] measured the angular distributions of the 92 keV and 530 keV lines in a nuclear alignment experiment. The anisotropy of the 530 keV line led to the prediction of spin 7/2 or 9/2 for the 530 keV level. The isotropic distribution of the 92 keV line was first understood as an attenuation effect due to the lifetime of

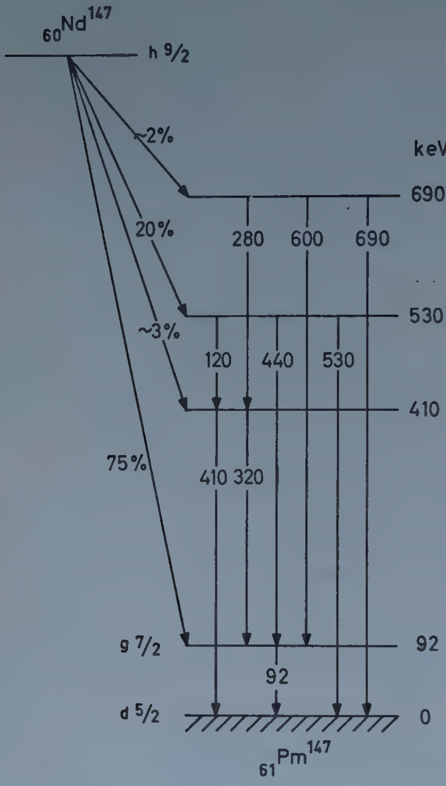

Fig. 8. Decay scheme of Nd^{147}.

that level. Later their opinion was revised [12] and the isotropy of the 92 keV line was interpreted as a result of mixing of the quadrupole and dipole radiations. For the mixing ratio $\delta = +0.17$ a complete isotropy is obtained.

Recently Bishop *et al.* [13] carried out a similar nuclear alignment experiment. They found anisotropic distributions for both the 530 keV line and the 92 keV line. From their results it was found that the spin of the 530 keV transition was $7/2+$ and that the 92 keV transition was a mixture of $M1$ and $E2$ with $\delta = -0.17 \pm 0.15$.

In order to throw some light on this discrepancy it was decided to carry out a gamma-gamma correlation experiment on the 320–92 keV cascade in Pm^{147}.

The Nd^{147} activity was obtained by bombarding neodymium oxide with thermal neutrons. Because of the simultaneous production of Nd^{149} ($T_{1/2} = 1.8$ h) and its daughter substance Pm^{149} ($T_{1/2} = 50$ h) the measurements started two weeks after the irradiation. The neodymium oxide was dissolved in alcohol and the solution was used in the correlation experiment.

The gamma spectrum in coincidence with the 92 keV line agreed with that found by Hans *et al.* [9]. By setting the discriminator channels on the respective photopeaks the contribution from other cascades can be neglected.

The anisotropies A and U were determined as follows according to eqs. (16) and (17):

$$A = -0.1099 \pm 0.0099, \qquad U = -0.0691 \pm 0.0099.$$

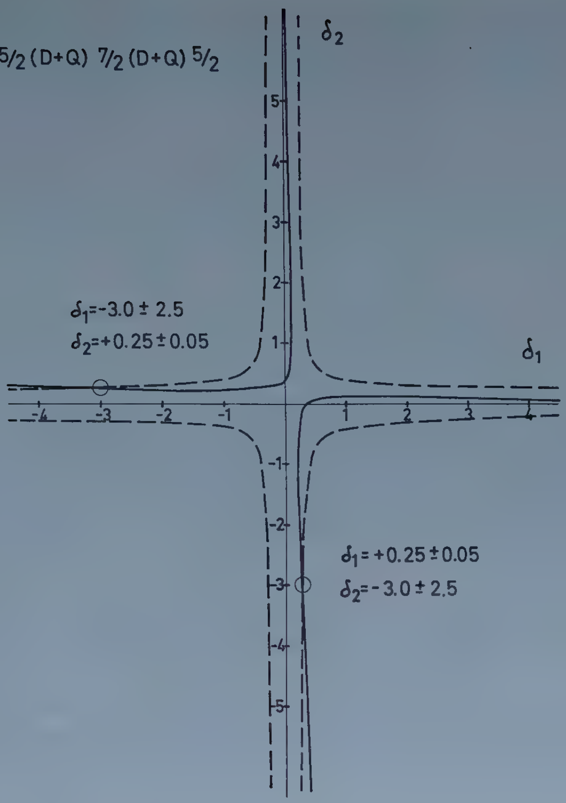

Fig. 9. The relations between the mixing parameters δ_1 and δ_2 in the spin sequence $5/2(D+Q)$ $7/2(D+Q)5/2$. $\delta_2=\phi_2(\delta_1)$ for A_2 (full line). $\delta_2=\phi_4(\delta_1)$ for A_4 (dashed line).

After correction for counter solid angle the following correlation function was obtained:

$$W(\theta)=1-(0.097\pm0.007)P_2(\cos\theta)+(0.023\pm0.018)P_4(\cos\theta).$$

Accordingly it can be settled that the 92 keV gamma transition is not isotropic which is in disagreement with Ambler *et al.* [11].

The 320–92 keV cascade can be described by the spin sequence j–7/2–5/2, where j is the spin of the 410 keV level. The positive sign of the A_4 coefficient is significant and excludes the following j-values: 3/2, 7/2 and 11/2. The spins 5/2 and 9/2 can both fit the correlation data. However, $j=9/2$ is very unlikely, because the beta group from $Nd^{147}(9/2-)$ to this level is of lower intensity than the beta group to the 530 keV level (7/2+). Thus it is concluded that the 410 keV level has spin 5/2. Accordingly the 320 keV transition might be a mixture of dipole and quadrupole radiations. The cascade can be described as $5/2(D+Q)7/2(D+Q)5/2$, with the mixing parameters δ_1 and δ_2, respectively.

With the experimentally determined A_2 and A_4 coefficients it is possible to obtain relations between δ_1 and δ_2. Fig. 9 shows $\delta_2=\phi_2(\delta_1)$ for A_2 (full line) and $\delta_2=\phi_4(\delta_1)$

for A_4 (dashed line). The intersections between the two functions define possible δ-values. One sees immediately that the functions are symmetric with respect to $\delta_1 = \delta_2$. Of the two intersections one can exclude the one with $\delta_2 = -3.0$, which should imply that the 92 keV transition is mostly $E2$. The other intersection gives

$$\delta_2 = +0.25 \pm 0.05.$$

It is therefore concluded that the 92 keV transition in Pm^{147} is

$$(94 \pm 2)\,\%\,M1 + (6 \pm 2)\,\%\,E2.$$

8. Discussion of the Ba^{131} and Nd^{147} results

The 122 keV transition in Cs^{131} and the 92 keV transition in Pm^{147} are both orbital momentum forbidden (l-forbidden) magnetic dipole transitions ($\Delta l = 2$, $\Delta j = 1$). It is therefore of interest to compare the mixing ratios with the single-particle model estimate as done by Lindqvist and Marklund [14] in the case of Tl^{203}.

According to Moszkowski [15] the transition rates of a single proton for $M1$ and $E2$ gamma transitions are

$$T(M1) = 2.8 \times 10^{13}(E_\gamma)^3 S(j_i L j_f), \tag{20}$$

$$T(E2) = 7.4 \times 10^{7}(E_\gamma)^5 \times A^{4/3} \times S(j_i L j_f), \tag{21}$$

where E_γ is the transition energy in MeV, $S(j_i L j_f)$ are statistical factors of the order of unity, and A the nuclear mass number. The nuclear radius is taken as $1.2 \times 10^{-13} \times A^{1/3}$ cm. The theoretical mixing parameter δ for such a transition is then obtained from

$$\delta^2_{\text{theor}} = \frac{T(E2)}{T(M1)}. \tag{22}$$

We now assume that in an l-forbidden transition the $M1$ transition rate is retarded by a factor defined in ref. [14] as the "retarding factor" R. It is further assumed that the $E2$ transition rate is not changed [16].

The experimentally determined mixing ratios for the l-forbidden transitions should then be

$$\delta^2_{\text{exp}} = \frac{T(E2)}{T(M1)\cdot R}, \tag{23}$$

or from (22) and (23)

$$R = \frac{\delta^2_{\text{theor}}}{\delta^2_{\text{exp}}}. \tag{24}$$

The results are shown in Table 2 together with the Tl^{203} result. The agreement between the three cases is fairly good. The retardations of l-forbidden magnetic dipole transitions thus found are somewhat stronger than found earlier [17]. It should be pointed out that the single particle estimate is actually expected to be good only in the case of Tl^{203}, which has one single proton hole within the closed shell of 82 protons.

Table 2. The retardation factor R for l-forbidden $M1$ transitions determined from correlation experiments in Cs^{131}, Pm^{147} and Tl^{203}.

Nucleus	E_γ MeV	Transition	R	Ref.
$_{55}Cs^{131}$	0.122	$g_{7/2} \rightarrow d_{5/2}$	$(0.9 \pm 0.1) \cdot 10^{-3}$	present work
$_{61}Pm^{147}$	0.092	$g_{7/2} \rightarrow d_{5/2}$	$(0.4 \pm 0.2) \cdot 10^{-3}$	present work
$_{81}Tl^{203}$	0.279	$d_{3/2} \rightarrow s_{1/2}$	$(1.3 \pm 2.7) \cdot 10^{-3}$	ref. [14]

9. Determination of nuclear *g*-factors

It was intended to measure the g-factors of the first excited states in Cs^{131} and Pm^{147} by studying the influence of an external magnetic field on the angular correlation. The lifetimes of the respective levels made such an attempt worth while.

The method of determining the g-factor of an intermediate level in a gamma cascade is described by Steffen [18]. Under the influence of an external magnetic field the angular correlation pattern is attenuated and simultaneously rotated by the angle $\omega \cdot \tau_b$, where ω is the Larmor frequency and τ_b is the lifetime of the intermediate level. The influence can be described by the following formula:

$$W(\theta, H) = \sum_\nu \frac{B_\nu}{1 + (\nu \omega \tau_b)^2} \left[\cos \nu \theta - \nu \omega \tau_b \sin \nu \theta \right], \tag{25}$$

where B_ν are the coefficients in the correlation function $W(\theta) = \sum B_\nu \cos(\nu \theta)$, and are thus related to A_ν in eq. (1). The magnitude of the g-factor can be determined from the attenuation, and the sign of g follows from the direction of rotation. The relation between the Larmor frequency ω, the g-factor and the magnetic field H is

$$\omega = g \cdot H \frac{\mu_N}{\hbar}, \tag{26}$$

where μ_N is the nuclear magneton.

In our experiment we used a water-cooled electromagnet, giving fields up to 30000 gauss. The angular correlation experiments with magnetic fields were carried out in a two-channel apparatus [19]. In order to avoid the influence of the magnetic field on the photomultipliers, it was necessary to introduce light guides between the NaI(Tl) crystals and the multipliers. Further, the multipliers were shielded with iron tubes (Fig. 10).

The experimental set up was tested by measuring the g-factor of the 482 keV level in Ta^{181} (Fig. 5). The lifetime of this level is 1.5×10^{-8} s. First the anisotropy A (eq. 3) for the 133–482 keV cascade in Ta^{181} was determined as a function of the magnetic field. In this experiment only the angles 180° and 90° were measured. Fig. 11 *b* shows the experimental results (not corrected for counter solid angle) and the theoretical curve for $|g| = 1.08$. In a second experiment the angular correlation pattern was investigated in more detail for zero field and for 7000 gauss. The following angles were measured: 135°, 157°5, 180°, 202°5, 225°, 247°5, and 270°. The result is shown in Fig. 11 *a*, where the experimental points are not corrected for counter solid angle. One sees immediately not only the attenuation but also the direction of the

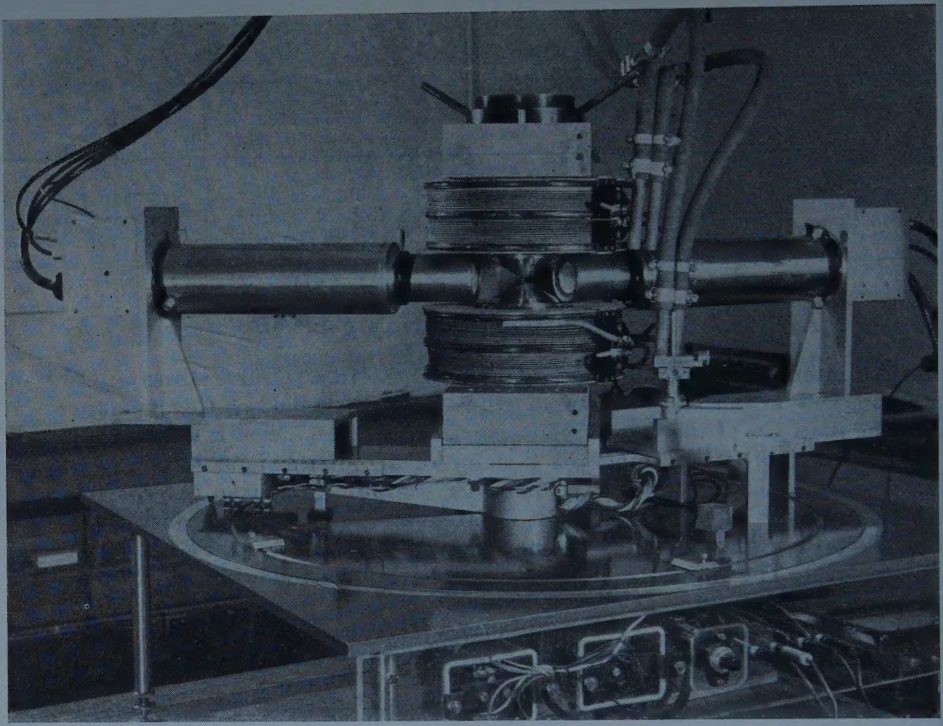

Fig. 10. Experimental set up for determination of nuclear g-factors.

rotation when the magnetic field is applied. From this experiment the sign of g was determined to be positive. The g-factor of the 482 keV level in Hf^{181} was thus measured to be

$$g = +1.08 \pm 0.10,$$

which is in good agreement with earlier measurements [20, 21].

In the case of Cs^{131} the anisotropy of the 496–122 keV cascade was too small (Chap. 7*b*) for a g-factor experiment.

The anisotropy of the 320–92 keV cascade in Pm^{147} was found to be $A = -0.110 \pm$ 0.010 (Chap. 7*c*), which is large enough for observing an attenuation. The lifetime of the 92 keV level was 3.5×10^{-9} s. However, even with a fairly high field, 2500 gauss, the attenuation was very small:

$$A\,(25000 \text{ gauss}) = -0.094 \pm 0.027.$$

Taking the limits of error into consideration it is possible to give only an upper limit of the g-factor in this case. It was not possible to measure the sign of g.

With eqs. (25) and (26) one obtains the following upper limit for the g-factor of the 92 keV level in Pm^{147}:

$$|g| \leq 1.0.$$

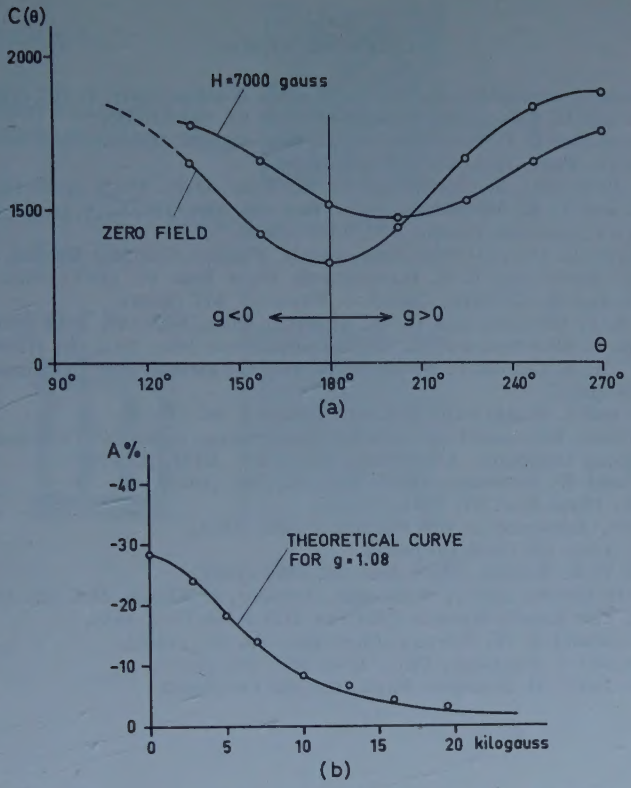

Fig. 11. The influence of a magnetic field on the angular correlation of the 133–482 keV cascade in Ta^{181}. (*a*) The correlation pattern for zero field and for 7000 gauss. (*b*) The anisotropy A as a function of the magnetic field.

The magnetic moment μ of a nuclear level can be obtained when both spin (I) and g-factor are known.

$$\mu = g \cdot I \cdot \mu_N. \tag{27}$$

The spin of the 92 keV level in Pm^{147} is 7/2 and therefore

$$\mu(g_{7/2}) \leq 3.5 \mu_N.$$

As a comparison it can be noted that the Schmidt value [22] for the corresponding level is

$$\mu = 1.7 \mu_N$$

and that the experimental values lie in the region

$$2.0 \mu_N \leq \mu \leq 3.0 \mu_N.$$

ACKNOWLEDGEMENT

The authors are indebted to Professor Kai Siegbahn for his interest in this work. Further thanks are due to Dr. T. R. Gerholm for advice in both experiments and in the treatment of data. We are also thankful to Mr. Åke Frisk for help in taking data.

REFERENCES

1. T. R. Gerholm, T. Lindqvist, and H. de Waard, Nuclear Instr. *1,* 107 (1957).
2. J. S. Lawson and H. Frauenfelder, Phys. Rev. *91,* 649 (1953).
3. F. K. McGowan and E. C. Campbell, Phys. Rev. *92,* 523 (1953).
4. F. K. McGowan, Phys. Rev. *93,* 471 (1954).
5. E. Heer, R. Rüetschi, F. Gimmi, and W. Kündig, Helv. Phys. Acta *28,* 336 (1955).
6. E. D. Klema and F. K. McGowan, Phys. Rev. *91,* 616 (1953).
7. H. Vartapetain, Comptes Rendus *243,* 1512 (1956).
8. H. Vartapetain, L. Dick, R. Foucher, and N. Perrin, Comptes Rendus *242,* 103 (1956).
9. H. S. Hans, B. Saraf, and C. E. Mandeville, Phys. Rev. *97,* 1267 (1955).
10. R. L. Graham and R. E. Bell, Canad. J. Phys. *31,* 377 (1953).
11. E. Ambler, R. P. Hudson, and G. M. Temmer, Phys. Rev. *97,* 1212 (1955).
12. E. Ambler, R. P. Hudson, and G. M. Temmer, Phys. Rev. *101,* 196 (1956).
13. G. R. Bishop, M. A. Grace, C. E. Johnson, H. R. Lemmer, and J. Perez y Jorba, Phil. Mag. *2,* 534 (1957).
14. T. Lindqvist and I. Marklund, Nuclear Physics *3,* 367 (1957).
15. S. A. Moszkowski, Beta and Gamma Ray Spectroscopy, editor Kai Siegbahn (North Holland Publishing Company, Amsterdam 1955), Ch. XIII, p. 373.
16. R. G. Sachs and N. Austern, Phys. Rev. *81,* 705 (1951).
17. A. B. Volkov, Phys. Rev. *94,* 1664 (1954).
18. R. M. Steffen, Advances in the Physics *4,* 293 (1955).
19. T. Lindqvist, Arkiv för Fysik (in press).
20. S. Raboy and V. E. Krohn, Phys. Rev. *95,* 1689 (1954).
21. E. Heer, R. Rüetschi, and P. Scherrer, Zeitschr. f. Naturf. *10a,* 834 (1955).
22. R. D. Evans, The Atomic Nucleus (McGraw Hill Book Co.), 1955.
23. D. E. Alburger and A. W. Sunyar, Phys. Rev. *99,* 695 (1955).
24. E. S. Snyder and S. Frankel, Phys. Rev. *106,* 755 (1957).
25. G. L. Keister and F. H. Schmidt, Phys. Rev. *93,* 140 (1954).

Tryckt den 26 september 1957

Uppsala 1957. Almqvist & Wiksells Boktryckeri AB